Synthesis and characterization of magnetic nano-sized Fe$_3$O$_4$ and CoFe$_2$O$_4$

D. Kovacheva[1]*, T. Ruskov[2], P. Krystev[2], S. Asenov[2], N. Tanev[2], I. Mönch[3], R. Koseva[3], U. Wolff[3], T. Gemming[3], M. Markova-Velichkova[1], D. Nihtianova[1], K.-F. Arndt[4]

[1] *Institute of General and Inorganic Chemistry, Bulgarian Academy of Sciences, 1113 Sofia, Bulgaria*
[2] *Institute for Nuclear Research and Nuclear Energy, 1784 Sofia, Bulgaria*
[3] *Leibniz Institute of Solid State and Materials Research Dresden, D-01069, Dresden, Germany*
[4] *Department of Chemistry, Physical Chemistry of Polymers, TU Dresden, D-0162, Dresden, Germany*

The synthesis of Fe$_3$O$_4$ and CoFe$_2$O$_4$ nanomaterials was performed by co-precipitation of corresponding metal hydroxides and their further decomposition to oxides under ultrasonic irradiation. The particles were characterized by X-Ray diffraction (XRD), transmission electron microscopy (TEM) and vibrating sample magnetometry (VSM). The crystallite sizes were 7.1 nm for the Fe$_3$O$_4$ sample and from 1.9 to 21 nm for the CoFe$_2$O$_4$ sample depending on the synthesis conditions. Mössbauer spectra of Fe$_3$O$_4$ and CoFe$_2$O$_4$ were measured at room temperature and 77 K. They revealed that samples show either superparamagnetic behavior or a mixture of superparamagnetism and ferrimagnetism depending on the crystallite sizes and temperature. Cation distribution for 10.4 nm CoFe$_2$O$_4$ was obtained from the Mössbauer spectra as well.

Key words: nanoparticle, spinel ferrites, sonochemical synthesis.

INTRODUCTION

Nano-sized materials made of magnetite (Fe$_3$O$_4$) and cobalt ferrite (CoFe$_2$O$_4$) are attractive both from fundamental point of view and for various physical, chemical and biological applications. The general formula of spinel ferrites is MO.Fe$_2$O$_3$ (where M is usually a divalent transition metal ion with an ionic radius, $r < 1$Å). The spinel ferrite structure consists of a cubic close-packed oxygen arrangement, in which cations occupy tetrahedral and octahedral interstices. Occupation of tetrahedral sites with divalent metal ions yields a normal spinel structure typical for M^{2+} = Zn^{2+}, Cd^{2+}, Mn^{2+}, while occupation of octahedral sites with divalent metal ions results in an inverse spinel structure when M^{2+} = Fe^{2+}, Co^{2+}, Ni^{2+}, Cu^{2+}. Ferrites comprise a broad and important class of magnetic materials, with important technological applications. Recently it was found that magnetic properties of nanosized spinel ferrites differ strongly from those of the corresponding bulk materials. For example magnetic saturation and coercitivity change drastically when the size of the particles becomes very small. Nanoparticle's physical and chemical characteristics are interesting not only from a fundamental point of view but also from a practical, since they offer possibilities for various new physical, chemical and biological applications. Special attention was paid to their application in medicine, where they can be used as magnetic resonance imaging agents in diagnostic, heat mediators in hyperthermia treatments as well as magnetic guidance for drug delivery [1–6].

Various synthetic methods have been developed to synthesize oxide nanoparticles, among them co-precipitation, thermal decomposition, sol-gel, microemulsion and other techniques [7–14]. It was established that the degree of crystallinity, particle size and particle morphology of oxide nanoparticles are strongly dependent on the method used for their preparation. The simplest synthetic procedure is based on the co-precipitation method, which involves the co-precipitation of M^{2+} and M^{3+} ions in basic aqueous media. Recently, the sonochemical method started to be applied widely in material science because it allows obtaining a wide range of functional materials such as magnetic nanocomposites, catalysts, molecular sieves etc. [15–18]. The mechanism of sonochemical reactions in aqueous and non-aqueous solutions is governed by two ma-

---

* To whom all correspondence should be sent:
E-mail: didka@svr.igic.bas.bg

jor effects accompanying the interaction of ultrasonic radiation with liquid media. The first one is the intensification of mass-transfer processes and the second one is cavitation. The collapse of cavitation bubbles results in an enormous rise of local temperatures and pressures leading to the decomposition of dissolved volatile compounds and the formation of amorphous and crystalline nanopowders.

In the present work we applied the sonochemical method for the synthesis of nanosize spinel oxide materials, namely Fe_3O_4 and $CoFe_2O_4$ samples with particle sizes in the range from 1.9 to 21 nm and investigated their size dependent structural and magnetic characteristics.

EXPERIMENTAL

The synthesis was performed by co-precipitation of corresponding metal hydroxides and their further decomposition to oxides under ultrasonic irradiation. As starting compounds $FeCl_2.6H_2O$, $Fe(NO_3)_3.9H_2O$, $Co(NO_3)_2.6H_2O$ and NaOH in a molar ratio of 1:2 were used. Metal nitrates and NaOH were dissolved separately in appropriate amount of distilled water. To obtain materials with different particle sizes for the $CoFe_2O_4$ samples the concentration of the initial solutions was varied. The co-precipitation took place while metal salt solutions were dropwise added to the solution of NaOH. The sonication of the precipitate was performed at 20 KHz, and 750 W in an ultrasonic processor SONIX, USA. The total sonication time was 1 hour. The obtained products were repeatedly washed with distilled water, filtered and finally dried at 50 °C.

Materials were first characterized by X-ray diffraction. Powder X-ray diffraction patterns were collected within the range from 10 to 80° 2θ with a constant step of 0.02° 2θ on a Bruker D8 Advance diffractometer with Cu Kα radiation and a LynxEye detector. Phase identification was performed with the Diffrac*plus* EVA using the ICDD-PDF2 Database. The powder diffraction patterns were evaluated with the Topas-4.2 software package using the fundamental parameters peak shape description including appropriate corrections for the instrumental broadening and diffractometer geometry. Unit cell parameters were obtained by whole powder XRD pattern fitting using as a starting values the data taken from the files in ICDD-PDF2 (#79-416 for magnetite and #70-8729 for $CoFe_2O_4$). Unit cell parameters, profile parameters as well as zero shift were varied to obtain a good fit with the experimental data. The mean crystallite domain sizes were determined using the same whole powder XRD pattern fitting mode of the program. For this purpose the integral line breadth approach for the

generalized treatment of the domain size broadening $-\beta_i = \lambda/L_{vol}\cos\theta$ was employed, where β_i is the integral breadth of the diffraction line i and L_{vol} is the volume weighted mean column height.

The specific surface area was determined by low temperature adsorption of nitrogen according to the B.E.T. method [19].

The particle size and morphology were determined using a TEM JEOL 2100 at 200 kV. The specimens are prepared by grinding the samples in an agate mortar and dispersing them in acetone by ultrasonic treatment for 6 min. A droplet of the suspension is dripped on standard carbon films on Cu grids. Additional crystal structure data are obtained using the selected area electron diffraction method (SAED). Particle size distributions were calculated on 100 to 200 particles in different images in bright field mode.

Magnetization measurements of the magnetite and $CoFe_2O_4$ samples were performed in a Quantum Design superconducting magnet system (PPMS) with vibrating sample magnetometer (VSM) option in fields up to 5 T at room temperature and 5 K.

[57]Fe Mössbauer measurements were performed using a constant acceleration spectrometer. A source of [57]Co(Rh) with an activity of 50 mCi was used. The Fe_3O_4 and $CoFe_2O_4$ spectra were taken in the transmission mode at room temperature and at liquid nitrogen temperature (77 K). The Mössbauer absorbers with a thickness of 40 mg cm^{-2} were made by mixing the studied nanomaterial powder with polyvinyl alcohol (glue material) and then pressed into disk pellets. Each experimental Mössbauer spectrum was decomposed either through the so-called "thin sample approximation" when the spectrum is represented as a sum of few simple spectra (sextets or doublets) or to avoid thickness effect it was fitted using an integral Lorentzian line shape approximation [20, 21]. When such decomposition is not possible one needs to take into account a distribution of spectra over a range of effective magnetic fields and/or electric field gradients. The geometric effect is taken into account as well.

RESULTS AND DISCUSSION

Figure 1 shows the XRD pattern of the nanosized magnetite material. The pattern was indexed within the cubic Fd-3m space group typical for the spinel structure. The unit cell parameter was measured to be 8.388(1) Å, which is closer to the value of 8.394 Å (ICDD-PDF2 #79-416 of crystalline magnetite (Fe_3O_4)), but differs from the unit cell parameter of maghemite 8.351 Å (ICDD-PDF2 #89-3850 cubic non-stoichiometric spinel γ-Fe_2O_3). The measured value for the unit cell parameter sug-
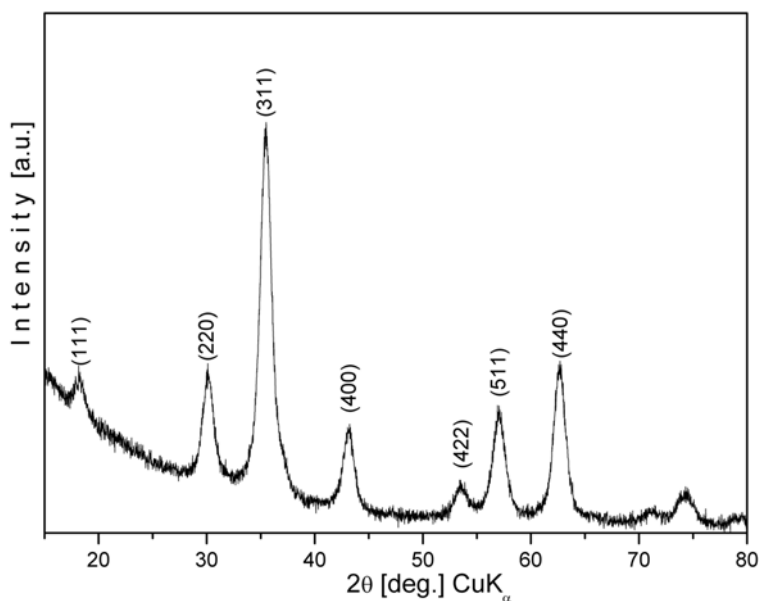
Fig. 1. XRD pattern of Fe_3O_4 with a particle size of 7.1 nm

gests a possibly non stiochiometric Fe^{2+}/Fe^{3+} ratio with some excess of Fe^{3+}. Analysis of the diffraction peak broadening resulted in a mean crystallite size of about 7.1 nm. This value agrees well with the high specific surface area of 180 m^2/g measured for this sample. Such high specific surface area corresponds to a mean particle size of 6.4 nm assuming not aggregated spherical particles. Powder diffraction patterns for $CoFe_2O_4$ samples synthesized from the same amount of initial compounds dissolved at different volumes are presented in Fig. 2. The corresponding mean crystallite sizes are shown in Table1.

Bright field TEM micrographs of Fe_3O_4 and $CoFe_2O_4$ samples together with the corresponding particle size distributions are presented in Fig. 3. Mean particle sizes obtained from TEM are given in Table 1. The spherical particles of Fe_3O_4 are distributed over a region from 3 to 11 nm. Polycrystalline SAED pattern of this sample shows that it is single phase and consists only of Fe_3O_4 (magnetite) ICDD-PDF2 #79-416. The spherical particles of $CoFe_2O_4$ with mean size of 2.7 nm (3.4 nm from XRD) are seen on Fig. 3b. It is worth to mention that these small particles produce a crystalline SAED pattern,
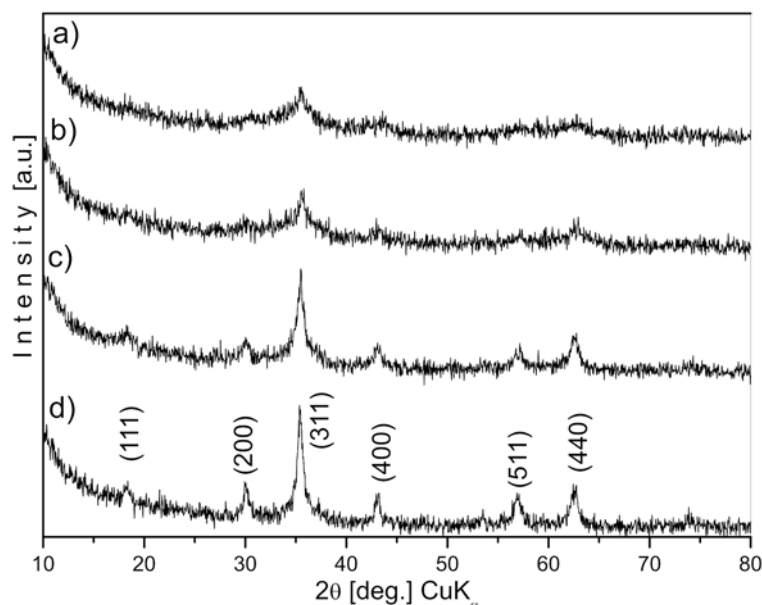
Fig. 2. XRD patterns of samples of $CoFe_2O_4$ obtained at different sonicated volumes: (a) – 300 ml, (b) – 200 ml, (c) – 100 ml and (d) – 50 ml

a)

b)

c)

d)
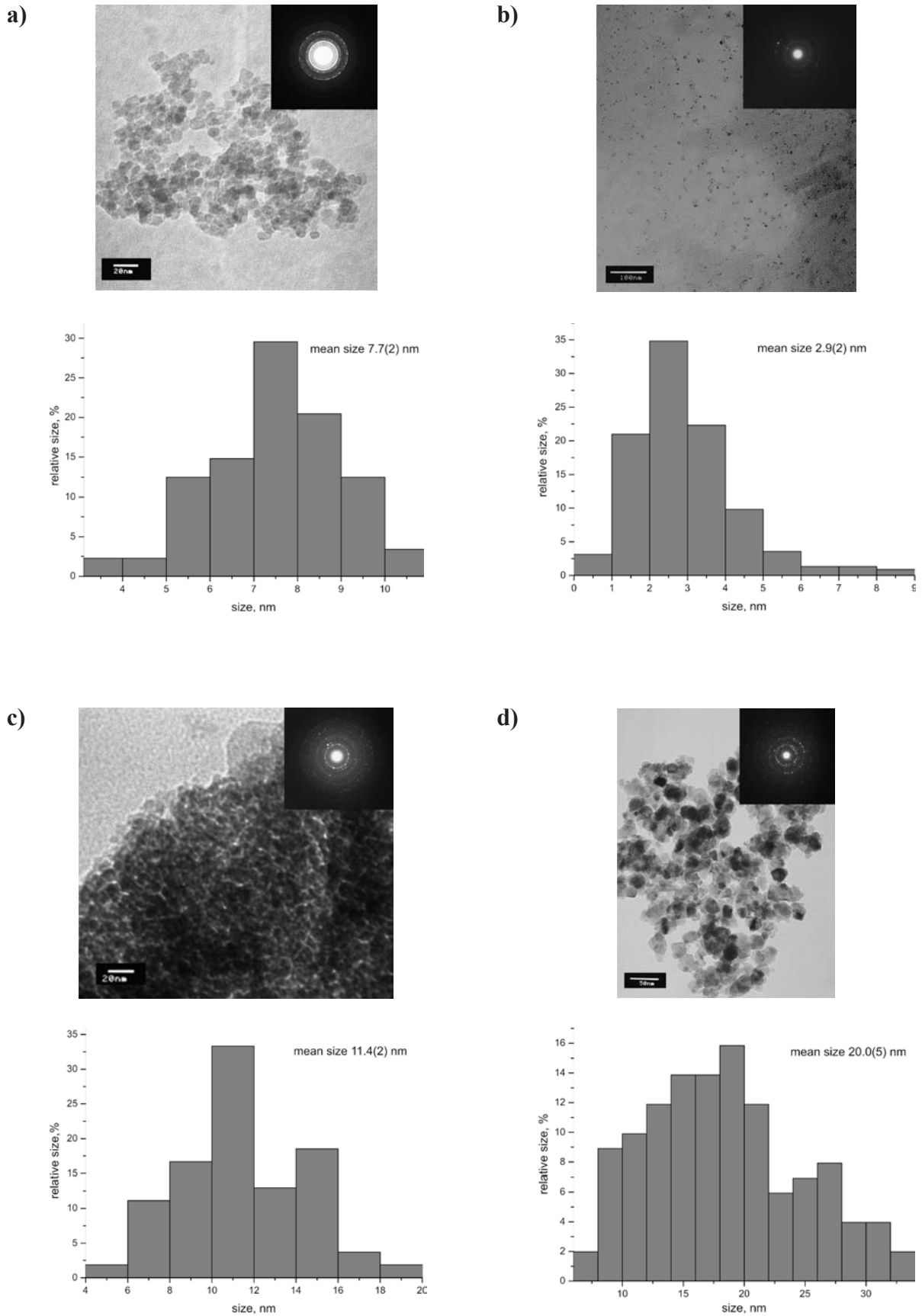
Fig. 3. TEM images and particle size distribution of (a) – Fe$_3$O$_4$ and CoFe$_2$O$_4$ obtained at different sonicated volumes: (b) – 200 ml, (c) – 100 ml and (d) – 50 ml

Table 1. Dependence of the coercitivity on the crystallite size of the samples

| Sample	Crystallite size [nm] XRD	Particle diameter [nm] TEM	Coercivity H_C [mT] at room temperature	Coercivity H_C [mT] at 5 K
Magnetite	7.1(2)	7.7(2)	70	
$CoFe_2O_4$	1.9(2)		0	
$CoFe_2O_4$	3.4(2)	2.9(4)	0	264
$CoFe_2O_4$	10.4(3)	11.4(2)	30	1157
$CoFe_2O_4$	21.0(5)	20.0(5)	105	

which corresponds to $CoFe_2O_4$ (spinel) phase ICDD-PDF2 #70-8729. On Fig. 3c and 3d we present spherical particles of $CoFe_2O_4$ samples with larger mean sizes. SAED patterns of these samples unambiguously show that they are crystalline and consist only of one phase: $CoFe_2O_4$ (spinel) ICDD-PDF2 #70-8729. For $CoFe_2O_4$ samples it can be seen that with increasing the mean size of the particles their distribution becomes wider.

Saturation magnetization M_s, remanent magnetization M_r, and coercivity H_c are the main technical parameters to characterize the magnetism of a ferromagnetic sample. The magnetization curves at room temperature of the magnetite sample and different $CoFe_2O_4$ samples are shown in Fig. 4a,b respectively. At room temperature the coercivity as well as the remanent magnetization of the $CoFe_2O_4$ samples is decreasing with smaller particle size (Table 1). The change of the magnetization of the nanoparticles (small particle sizes) follows spontaneously the orientation of the applied magnetic field. The samples with the smallest particle size of 1.9 and 3.4 nm exhibit a complete superparamagnetic behaviour (Fig. 4b), which was also confirmed by Mössbauer spectroscopy (Fig. 7a). $CoFe_2O_4$ nanoparticles show typical hysteresis for their field-dependent magnetization below the blocking temperature. Fig. 5 is showing the hysteresis curves of two $CoFe_2O_4$ samples with a particle size of 3.4 and 10.4 nm measured at 5 K. The magnetization of the nanoparticles is not following the applied magnetic field simultaneously, but has to overcome a certain magnetic field value. This coercive field represents the value which is needed to surpass the anisotropy barrier [22–24]. Therefore, the coercivities for the $CoFe_2O_4$ samples strongly increased with lower temperature. The measurements show clearly that the coercivity H_c is strongly size and temperature dependent [25, 26].

The Mössbauer spectrum of nanosized magnetite (Fe_3O_4) taken at room temperature is shown in Fig. 6a. The extremely broadened six lines indicate that the sample consists of a mixture of superparamagnetic and ferrimagnetic phases rather than a
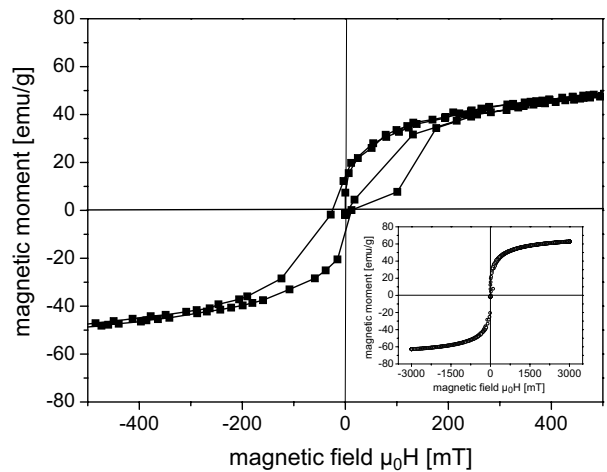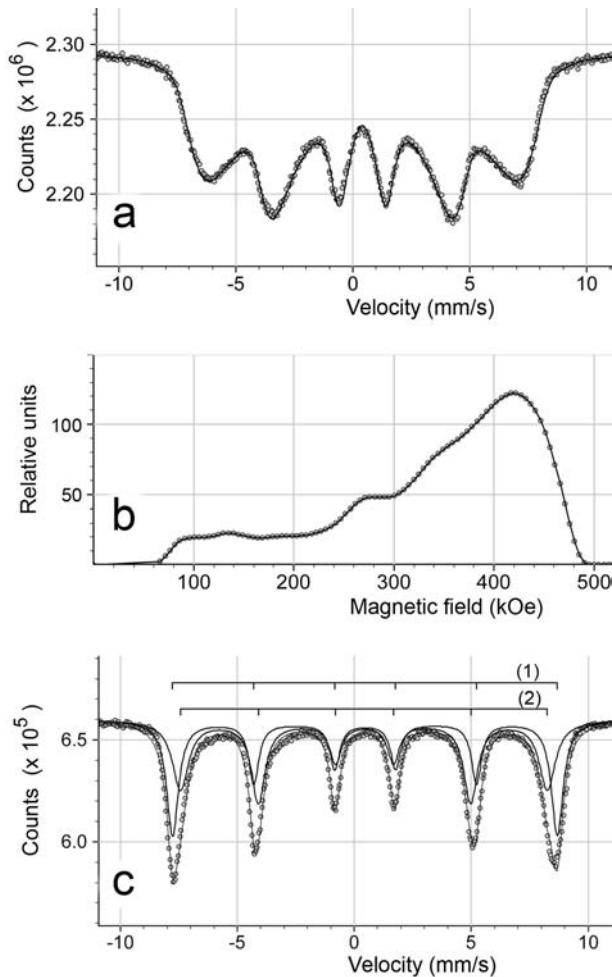

Fig. 4a) Room temperature magnetization curve of Fe_3O_4 (7 nm). The majority of particles are in an intermediate region (between the superparamagnetic and ferromagnetic state). The inset shows the hysteresis curve measured up to ± 3 T
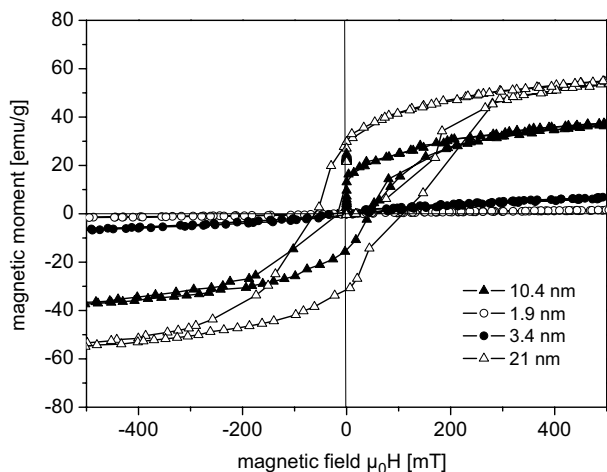
Fig. 4b) Magnetization curves of $CoFe_2O_4$ nanoparticles, measured at room temperature: 1.9 nm – open circles, 3.4 nm – filled circles, 10.4 nm – filled triangles, and 21 nm – open triangles. The first two groups of nanoparticles are completely in the superparamagnetic state, while the third and the fourth are in an intermediate region of a mixed superparamagnetic and ferrimagnetic state
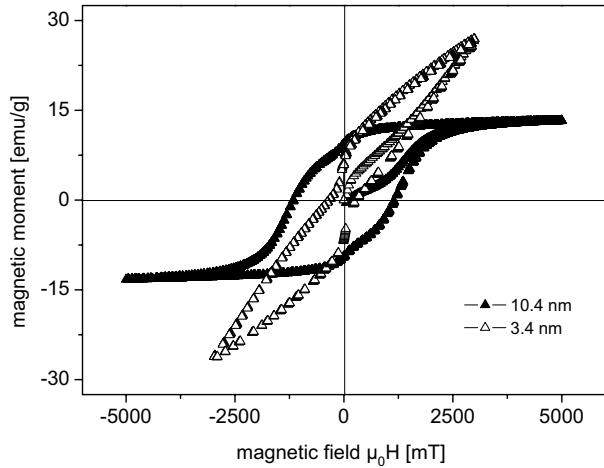
Fig. 5. Hysteresis loops at 5 K for $CoFe_2O_4$ samples with a particle size of 3.4 nm – open triangles and 10.4 nm – filled triangles

pure superparamagnetic. The spectrum was fitted as a magnetic sextet's distributions of 100 closely spaced sextets with a hyperfine magnetic field distribution (Fig. 6b). The average isomer shift and hyperfine magnetic field are: IS=0.41 mm/s and H = 364 kOe. The Mössbauer spectrum of the same sample at liquid nitrogen temperature (Fig. 6c) was fitted as a superposition of two magnetic sextets. At this temperature the superparamagnetic relaxations are blocked for the majority of the magnetic nanoparticles, however the broadening of the resonance lines for both sextets still could be explained as small influence of the superparamagnetism. The isomer shifts for sextets (1) and (2) are 0.46 mm/s and 0.38 mm/s respectively showing that the Fe^{2+} in the magnetite sample is partially oxidized to Fe^{3+}, forming some part of maghemite (γ-Fe_2O_3). The hyperfine magnetic fields derived from the sextets (1)

Fig. 6. Mössbauer spectrum of Fe_3O_4 taken at room temperature – fitted as a magnetic sextet's distribution (a); the hyperfine magnetic field distribution (b); Mössbauer spectrum of the sample taken at 77 K – fitted as a superposition of two magnetic sextets (c)
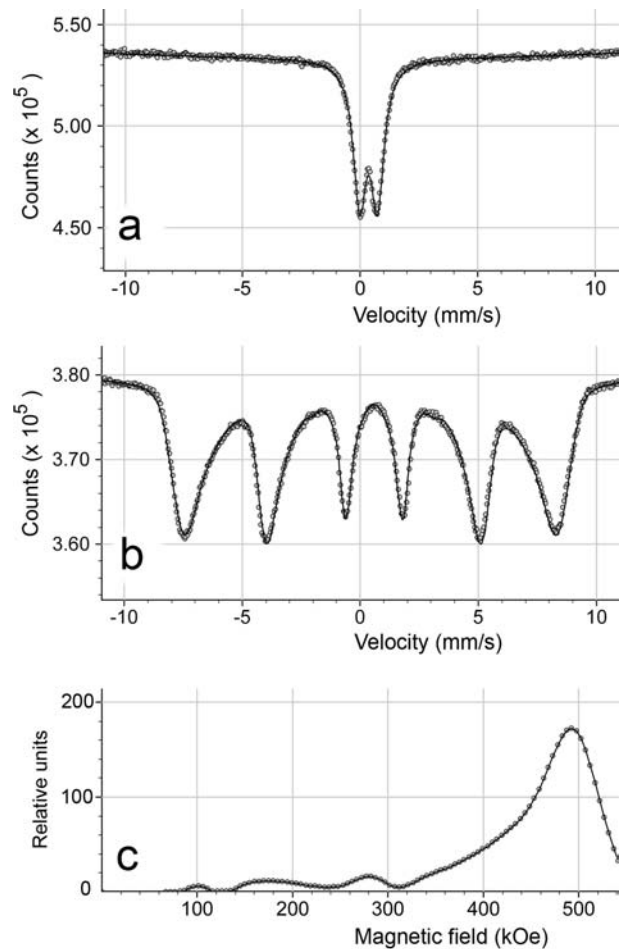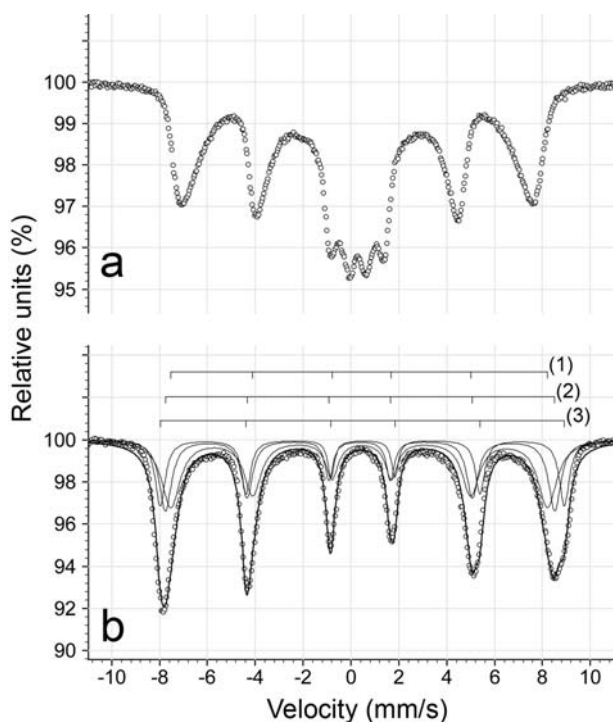

Fig. 7. Mössbauer spectrum of $CoFe_2O_4$ (3.4 nm) taken at room temperature – fitted as a quadrupole doublet (a); Mössbauer spectrum of the same sample taken at 77 K – fitted as a magnetic sextet's distribution (b); the hyperfine magnetic field distribution (c)

and (2) are 511 kOe and 487 kOe respectively. On the basis of these data and taking into account the Mössbauer data for 6.2 nm magnetite (Fe_3O_4) obtained by A. D. Arelaro et al. [27] we could assign the sextet (1) to Fe^{3+} in octahedral (B-site) and the sextet (2) to Fe^{3+} in tetrahedral (A-site).

In Fig. 7a the Mössbauer spectrum of $CoFe_2O_4$ (3.4 nm) at room temperature is shown. The superparamagnetic behavior of these nanoparticles leads to a complete lack of magnetic hyperfine splitting of the spectrum and represents a quadrupole doublet with broadened lines with an isomer shift of 0.36 mm/s and a quadrupole splitting of 0.76 mm/s. The origin of the quadrupole doublet line broadening is connected with the surface of the particle and the layers in the immediate vicinity of the surface, creating different electric field gradients on the Fe nucleus as compared to the electric field gradient from the core of the nanoparticle.

The Mössbauer spectrum of $CoFe_2O_4$ (3.4 nm) taken at 77 K represents a sextet with broadened lines (Fig. 7b). The fluctuations of the magnetization direction are partially blocked and the magnetic hyperfine splitting takes place. The spectrum was fitted as a magnetic sextet's distribution of 100 sextets with a hyperfine magnetic field distribution with an average magnetic hyperfine field of 442 kOe (Fig. 7c).

Fig. 8 shows the Mössbauer spectra of $CoFe_2O_4$ (10.4 nm) taken at room temperature (a) and at 77 K (b) respectively. The RT spectrum (a) shows a high percentage of superparamagnetic behavior of the sample, and therefore it is not possible to extract information about the cation distribution from such a spectrum. In contrast, the second spectrum (b), taken at 77 K, shows that the contribution of the superparamagnetic component is negligible and the spectrum can be fitted quite well with three magnetic sextets. The isomer shifts for the sextets (1), (2), and (3) are 0.37 mm/s, 0.49 mm/s and 0.39 mm/s, respectively. The hyperfine magnetic fields derived from the sextets (1), (2), and (3) are 489 kOe, 505 kOe, and 524 kOe, respectively. From these parameters one can conclude that sextet (1) corresponds to the Fe^{3+} cation in A-site, while the sextets (2) and (3) correspond to Fe^{3+} placed in B-site (B2 and B3). From the measured relative spectral areas of the sextets (1), (2), and (3) we can derive the formula for the cation distribution of $CoFe_2O_4$ (10.4 nm), namely: $(Co_{0.1}Fe_{0.9})[Co_{0.9}Fe_{1.1}]O_4$. Possible explanation for the two octahedral sites B2 and B3 is given in the paper of Lopes et al. [28] where the Mössbauer spectrum for cobalt ferrite nanoparticles (7.2 nm), taken at 5 K was fitted with three subspectra related to Fe^{3+} in A-site and Fe^{3+} in B2 and B3-sites. The two B-sites correspond to different surroundings of Fe^{3+} in the B-positions of the spinel structure.

CONCLUSIONS

Nanoparticles of two different ferrite materials, Fe_3O_4 and $CoFe_2O_4$, have been obtained by ultrasound assisted co-precipitation. The method allows producing oxide materials with a preliminary desired mean particle size within the nanoscale range by simple control of synthesis governing parameters, such as reactant concentration, power input and reaction time. Magnetic measurements at room temperature and 5 K have shown that the magnetization behaviour changes clearly with temperature. At room temperature the $CoFe_2O_4$ samples with the smallest particle size of 1.9 and 3.4 nm exhibit a complete superparamagnetic behaviour, while samples with bigger particles show a mixed state of superparamagnetic and ferrimagnetic behaviour. Mössbauer spectroscopy measurements provide the formula for cation distribution of $CoFe_2O_4$ (10.4 nm), namely $(Co_{0.1}Fe_{0.9})[Co_{0.9}Fe_{1.1}]O_4$.

Fig. 8. Mössbauer spectra of $CoFe_2O_4$ (10.4 nm) taken at room temperature (a), and taken at 77K and fitted as a superposition of three magnetic sextets (b)

REFERENCES

1. L. Babes, B. Denizot, G. Tanguy, J. Le Jeune, P. Jallet, *J Colloid Inter Sci*, **212**, 474 (1999).
2. I. Safarik, M. Safarikova, *Monats Chem*, **133**, 737 (2002).
3. Q. Pankhurst, J. Connolly, S. Jones, J. Dobson, *J Phys D: Appl Phys*, **36**, 167 (2003).
4. X. Wang, H. Gu, Zh. Yang, *J Magn Magn Mater*, **293**, 334 (2005).
5. M. Lin, H. Kim, H. Kim, M. Muhammed, K. Kim Do, *Nano Reviews*, **1**, 4883 (2010).
6. A. Figuerola, R. Di Corato, L. Manna, T. Pellegrino, *Pharmacological Research*, **62**, 126 (2010).
7. K. Haneda, A. Morrish, *J de Physique*, **38**, C1-321 (1977).
8. T. Hosono, H. Takahashi, A. Fijita, R. Justin Joseyphus, K. Tohji, B. Jeyadevan, *J Magn Magn Mater*, **321**, 3019 (2009).
9. V. Blaskov, V. Petkov, V. Rusanov, Li. Martinez, B. Martinez, J. Monos, M. Mikhov, *J Magn Magn Mater*, **162**, 331 (1996).
10. P. Sraravanan, S. Alam, G. Mathur, *J Mater Sci Lett*, **22**, 1283 (2003).
11. D. Maity, S. Kale, R. Kaul-Ghanekar, Xue Jun-Min, J. Ding, *J Magn Magn Mater*, **321**, 3093 (2009).
12. Z. Hua, R. Chen, C. Li, S. Yang, M. Lu, B. Gu, Y. Du, *J Alloys Comp*, **427**, 199 (2007).
13. M. Liu, X. Li, H. Imrane, Y. Chen, T. Googrich, Z. Cai, K. Ziemer, J. Huang, N. Sun, *Appl Phys Lett*, 152501 (2007).
14. S. Santra, R. Tapes, N. Theodoropoulou, J. Dobson, A. Hebard, W. Tan, *Langmuir*, **17**, 2900 (2001).
15. J. Bang, K. Suslick, *Adv Mater*, **22**, 1039 (2010).
16. I. Ray, S. Chakraborty, A. Chowdhury, S. Majumdar, A. Prakash, R. Pyare, A. Sen, *Sensors and Actuators B*, **130**, 882 (2008).
17. E. Kim, H. Lee, H. Shao, *Key Eng Mater*, **277-279**, 1044 (2005).
18. S. Park, J. Kim, C. G. Kim, C. O. Kim, *Current Appl Phys*, **8**, 784 (2008).
19. S. Brunauer, H. Emmett, E. Teller, *J. Am. Chem. Soc.*, **60**, 309 (1938).
20. G. Shenoy, J. Friedt, H. Maleta, S. Ruby, *Mössbauer Effect Methodology*, **9**, 277 (1974).
21. T. Cranshaw, *J Phys E*, **7**, 122 (1974).
22. S. Laureti, G. Varvaro, A. M. Testa, D. Fiorani, E. Agostinelli, G. Piccaluga, A. Musinu, A. Ardu, D. Peddis, *Nanotechnology*, **21**, 315701 (2010).
23. Ch. Liu, Z. J. Zhang, *Chem. Mater.*, **13**, 2092 (2001).
24. Ch. Liu, B. Zou, A. J. Rondinone, Z. J. Zhang, *J. Am. Chem. Soc.*, **122**, 6263 (2000).
25. G. Herzer, *IEEE Trans Mag*, **26**, 1397 (1990).
26. G. Herzer, *J Magn Magn Mater*, **112**, 258 (1992).
27. A. Arelaro, L. Rossi, H. Rechenberg, *Journal of Physics: conference series*, **217**, 012126 (2010).
28. J. L. Lopez, H. D. Pfannes, R. Paniago, J. P. Sinnicker, M. A. Novak, *J Magn Magn Mater*, **320**, e327 (2008).

СИНТЕЗ И ХАРАКТЕРИЗИРАНЕ НА МАГНИТНИ НАНОРАЗМЕРНИ Fe₃O₄ И CoFe₂O₄

Д. Ковачева[1], Т. Русков[2], П. Кръстев[2], С. Асенов[2], Н. Танев[2], И. Мьонж[3], Р. Косева[3], У. Волф[3], Т. Геминг[3], М. Маркова-Величкова[1], Д. Нихтянова[1], К.-Ф. Арндт[4]

[1] *Институт по обща и неорганична химия, Българска академия на науките, 1113 София, България*

[2] *Институт за ядрени изследвания и ядрена енергетика, 1784 София, България*

[3] *Лайбниц институт за изследвания на твърдо състояние и материали, Дрезден, D-01069, Дрезден, Германия*

[4] *Катедра по химия, Физикохимия на полимери, ТУ - Дрезден, D-0162, Дрезден, Германия*

(Резюме)

Синтезът на наноразмерните Fe₃O₄ и CoFe₂O₄ бе проведен чрез съутаяване на съответните метални хидроксиди и тяхното по-нататъшно разлагане до оксиди под въздействие на ултразвуково облъчване. Получените материали са характеризирани с рентгенова дифракция (XRD), трансмисионна електронна микроскопия (ТЕМ) и вибрационна магнитометрия (VSM). Получените материали са със средни размери на кристалитите 7.1 нанометра за Fe₃O₄ проба и от 1.9 до 21 нанометра при CoFe₂O₄ проби в зависимост от условията на синтез. Мьосбауеровите спектри на Fe₃O₄ и CoFe₂O₄, измерени при стайна температура и 77 K показаха, че пробите проявяват или суперпарамагнитно поведение или смес от суперпарамагнитно и феримагнитно в зависимост от на размера на кристалитите и температурата. Чрез Мьосбауеровата спектроскопия е определено и катионното разпределение за образец от CoFe₂O₄ с размер на кристалитите 10.4 nm.